Electronic Supplementary Material (ESI) for Journal of Materials Chemistry C.

Supporting Information

Dual-enhanced Raman Scattering Sensors Incorporating Graphene Plasmonic Nanoresonators

Xiaoqiang Feng[a], Zhengyi He[a], Lingyan Yu[a], Zhiduo Liu[b], Gang Wang[a,*], Siwei Yang[c,*], and Guqiao Ding[a,c]

[a]Department of Microelectronic Science and Engineering, School of Physical Science and Technology, Ningbo University, Ningbo 315211, P. R. China.

[b]State Key Laboratory of Integrated Optoelectronics, Institute of Semiconductors, Chinese Academy of Sciences, Beijing 100083, P. R. China.

[c]State Key Laboratory of Functional Materials for Informatics, Shanghai Institute of Microsystem and Information Technology, Chinese Academy of Sciences, Shanghai 200050, P. R. China.

*Correspondence to: gangwang@nbu.edu.cn (G. Wang); yangsiwei@mail.sim.ac.cn (S. Yang)

1. VAGAs height

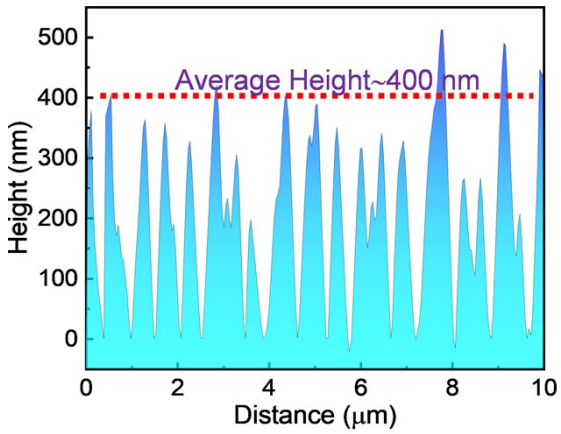

Fig. S1 The height curves of VAGAs.

2. Porosity of 2D-Gr

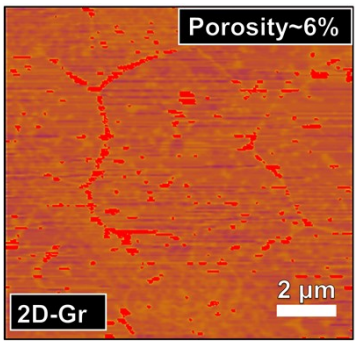

Fig. S2 The Porosity of 2D-Gr is about 6%.

3. Porosity of different heights

We characterized the porosity of VAGA with different heights, and found that the VAGA has the maximum porosity when the height of the VAGA is 400 nm, and the adsorption effect on the molecules is the best at this time.

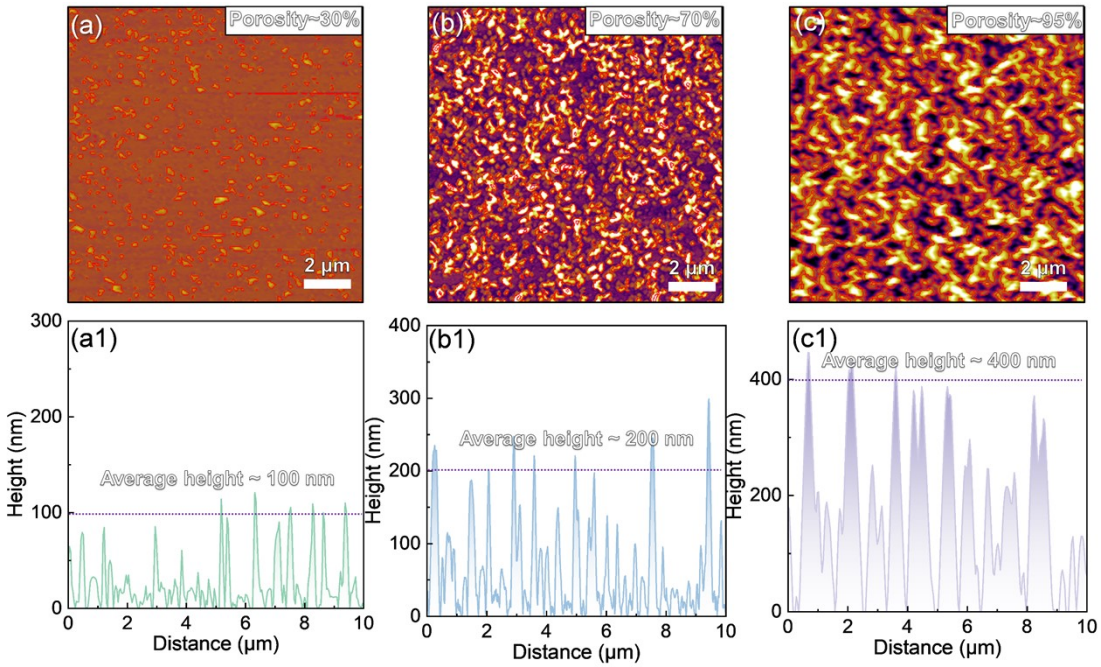

Fig. S3 Porosity of different heights. (a, a1) Porosity of VAGA at a height of 100 nm. (a) indicates its porosity, (a1) indicates the corresponding VAGA height. (b, b1) Porosity of VAGA at a height of 200 nm. (b) indicates its porosity, (b1) indicates the corresponding VAGA height. (c, c1) Porosity of VAGA at a height of 400 nm. (c) indicates its porosity, (c1) indicates the corresponding VAGA height.

4. The influence of different porosity on SERS performance

We used 10^{-6} M R6G to characterize SERS substrates made of VAGA with different heights, and found that when the height of VAGA is 400 nm, the SERS performance is the best.

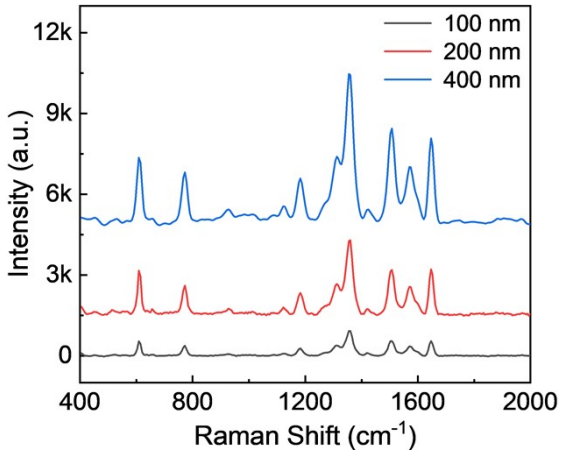

Fig. S4 SERS performance of VAGA at different heights.

5. The abs of the three structures

We tested the absorbance (abs) of the three structures (FTO, 2D-Gr/FTO, VAGA/FTO), and their abs increased sequentially, as shown Fig. S5.

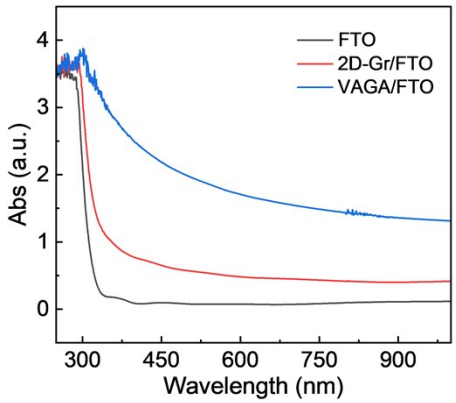

Fig. S5 The abs of the three structures of FTO, 2D-Gr/FTO, VAGA/FTO.

6. Raman diagrams of 2D-Gr and VAGA

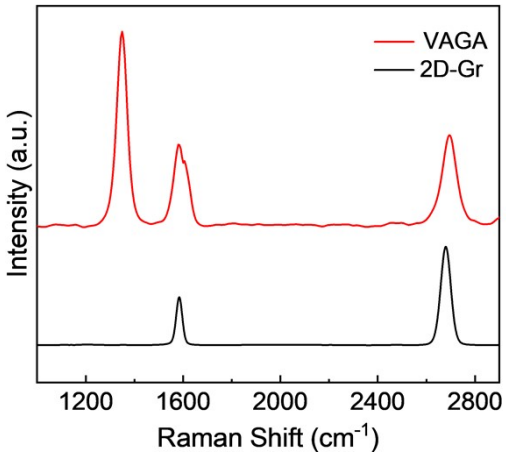

Fig. S6 Raman diagrams of 2D-Gr and VAGA.

7. The crystallinity of VAGA affects the performance of SERS

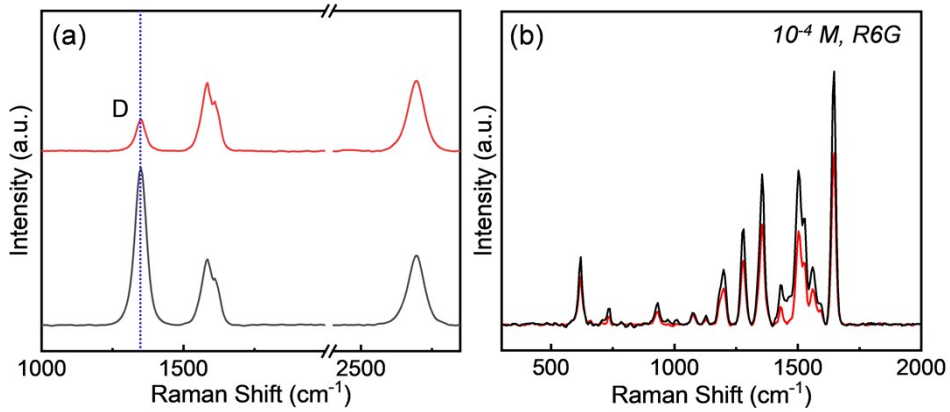

Fig. S7 (a) The Raman diagram of highly crystalline of VAGA (red line) and lowly crystalline of VAGA (dark line). (b) The SERS performance of 10^{-4} M R6G with highly (red line) and lowly (dark line) crystalline VAGA, respectively.

8. The SERS effect of the VAGAs/FTO and FTO substrates

Fig.S8 shows the SERS spectra of 10^{-6} M R6G, 10^{-6} M RB, and 10^{-6} M MB using FTO and VAGAs/FTO as substrate, respectively. The SERS effect can be observed on both of FTO and VAGAs/FTO, as shown in Fig. S8a-c. The enhancement factors of VAGAs/FTO SERS substrate for R6G (1360 cm^{-1}), RB (1626 cm^{-1}), and MB (1647 cm^{-1}), are estimated to be 142, 41, and 12, respectively, as shown in Fig. S8d.

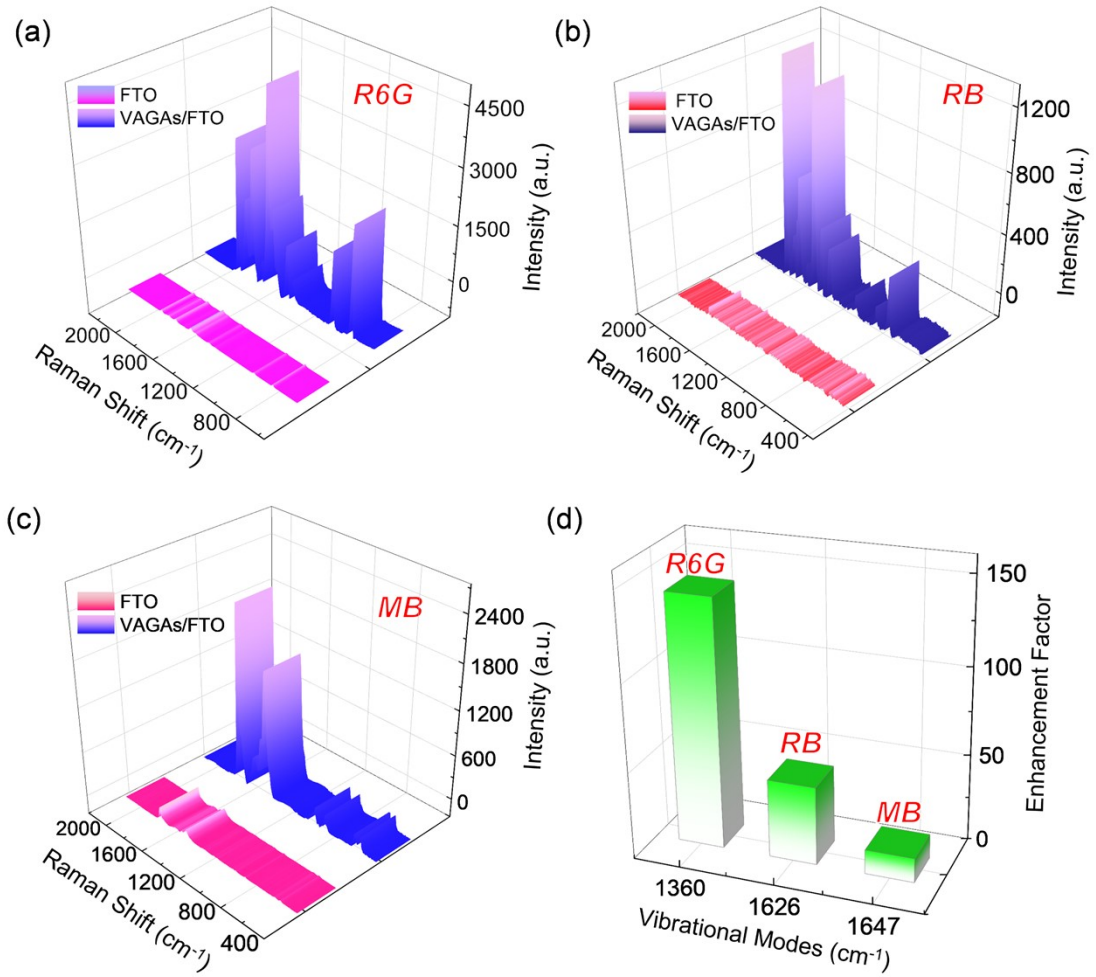

Fig. S8 SERS spectra of (a) 10^{-6} M R6G, (b) 10^{-6} M RB (e) 10^{-6} M MB. (d) Enhancement factor calculation of specific vibrational modes corresponding to each analyte.

9. Repeatability of VAGA after washing 8 times

We processed the Raman mapping of the VAGA after eight washings. The results show that the VAGA still has good reproducibility after washing.

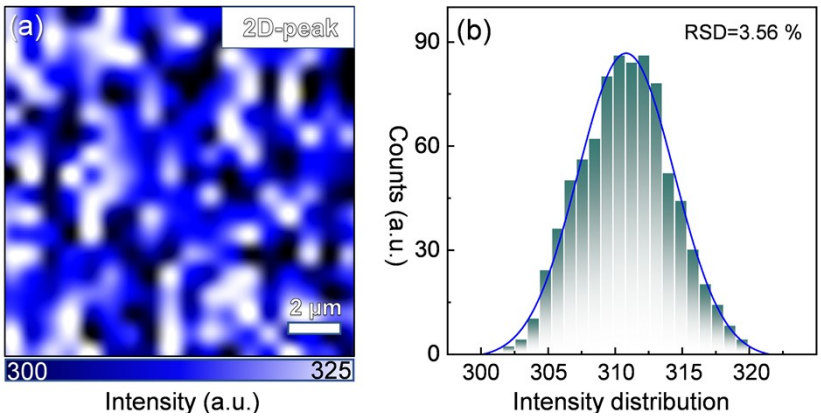

Fig. S9 (a) Raman mapping of the peak at 2D-peak for VAGA after washing 8 times. (b) The corresponding distribution of the Raman intensities.

10. Topography of glass and FTO

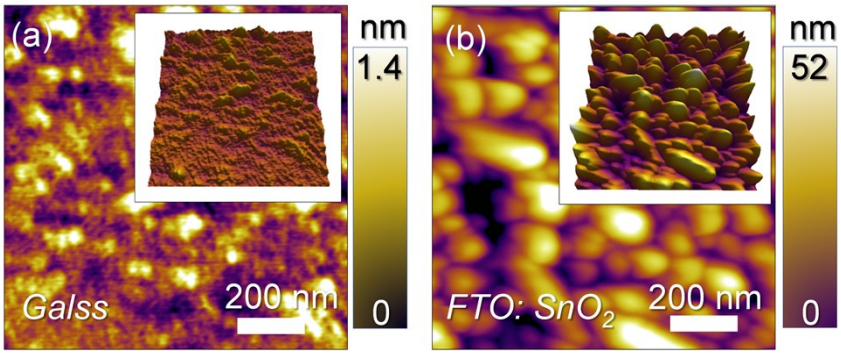

Fig. S10 (a) AFM topography of glass, the illustration shows the 3D shape. (b) AFM topography of FTO, the illustration shows the 3D shape.

11.The rate of "rapid electron transfer"

The improvement of SERS performance is inseparable from the rate of rapid electron transfer. The overall process involves ballistic electron injection followed by hot electron relaxation to form band-edge polarons then Drude-like transport back to the surface under the action of the interfacial electric field. Hot electron relaxation in ionic semiconductors such as SnO_2 is dominated by the emission of polar optical (LO) phonons.[1] The ballistic mean free path, λ_b, of an electron travelling in rutile perpendicular to the optical axis and having excess energy E^{ex} is given by,[2]

$$\lambda_b = <\tau_b> \times \nu_b$$

$$=<\tau_b> \times \left(\frac{2E^{ex}}{m^*_\perp}\right)^{1/2},$$

where τ_b is the mean scattering time, ν_b is the velocity of the ballistic electron, and $m^*_\perp = 1.2\ m_e$ is the electron band mass.[3] A discrete flux of electrons crossing the surface will establish an energetically relaxed band-edge electron (polaron) density distribution of the form $n = n_0 \exp(-z/\lambda_b)$, where n is the local number concentration of electrons (polarons) and z is the coordinate in the surface normal direction, with z=0 at the surface and positive values of z increasing within the bulk of the crystal. The electron (polaron) population will drift back toward the interface under the action of the interfacial electric field where electron transfer back to the nanocrystal film reduces the total amount of separated charge, given by,[2]

$$Q^{sep} = Ae \int_{z=0}^{z=\infty} n(z,t)dz$$

Upon integration, we find that the total amount of separated charge decreases over time according to,[4]

$$Q^{sep} = Q_0 \exp(-\nu_p t/\lambda_b)$$

Where $\nu_p = \mu \mathbf{E}$ is the polaron drift velocity and μ is the polaron mobility. A typical polar optical scattering time of $\tau_b = 50$ fs and hot electron excess energy of $E^{ex} = 0.2$ eV lead to a ballistic mean free path of $\lambda_b = 12$ nm. The fast electron transfer rate is about 120

$cm^2\ V^{-1}\ s^{-1}$.

References

1 K. F. Brennan, The Physics of Semiconductors (Cambridge University Press, 1999).

2 N. Bloembergen, C. H. Lee, *Phys. Rev. Let*t. 1967, **19**, 835.

3 K. M. Glassford, J. R. Chelikowsky, *Phys. Rev. B* 1992, **46**, 1284.

4 B. Dick, A. Gierulski, G. Marowsky, G. A. Reider, *Appl. Phys. B* 1985, **38**, 107.